BNL-101984-2014-TECH

AD/RHIC/72;BNL-101984-2013-IR

Betatron Distortion Due to Linear Coupling and its Effects on the Dynamic Aperture in RHIC

G. Parzen

June 1990

Collider Accelerator Department

Brookhaven National Laboratory

U.S. Department of Energy

USDOE Office of Science (SC)

DISCLAIMER

AD/RHIC–72

RHIC PROJECT

Brookhaven National Laboratory
Associated Universities, Inc.
Upton, NY 11973

Betatron Distortion Due to Linear Coupling and its Effects on the Dynamic Aperture in RHIC

G. Parzen

June 1990

Betatron Distortion due to Linear Coupling and its Effects on the Dynamic Aperture in RHIC

G. Parzen

1. Introduction

The coupling introduced by the random a_1 can produce considerable distortion of the betatron motion. For a given initial x_o, x'_o, y_o, y'_o, maximum x and the maximum y for the subsequent motion can be considerably larger when coupling is present. The maximum x and y can be used as a measure of the betatron distortion.

One effect of this betatron distortion shows up in the dynamic aperture, in a loss in the stability limit, A_{SL}, found by tracking. The betatron distortion causes the particle to move further out in the magnets, where it sees stronger non–linear fields. The betatron distortion effect also shows up in a loss of linear acceptance. In injection and extraction, the larger betatron motion caused by the coupling requires more aperture.

Previous tracking[1] showed a loss in A_{SL} due to random a_1 and b_1. It was noticed then that the loss in A_{SL} was associated with a betatron motion distortion which was primarily a linear effect. For a given initial x, x', y, y' the $x_{\max}$ and $y_{\max}$ in the high–β magnets were considerably larger (about 30% larger) for those random a_1 distributions which produced the smaller A_{SL}.

The studies described below show that the stability limit, A_{SL}, depends on the starting location around the ring. This variation in A_{SL} around the ring can be correlated with the variation in the betatron distortion for particles starting at different places around the ring. It is proposed that the average of the A_{SL} found by starting at each of the QF, the focusing quadrupoles in the arcs, can be taken as a measure of the dynamic aperture. It was found that the average A_{SL} is reduced by about 15% by the random a_1 multipoles expected in RHIC.

2. β–Functions of the Normal Modes

Edwards and Teng showed how to transform to a new set of coordinates v, v', u, u' which are uncoupled.[2] These new normal coordinates are related to x, x', y, y' by a 4×4 matrix R

$$x = R \ v \ .$$

---

[1] G. Parzen, AD/RHIC–AP–80, 1989.

[2] D. Edwards and L. Teng, IEEE 1973 PAC, p. 885.

The normal coordinates have emittances ϵ_1 and ϵ_2 and β–functions β_1 and β_2. ϵ_1 and ϵ_2 are invariants. The x and y motion can be written as the sum of these two normal modes.

β_1 and β_2 and the R matrix can be computed from the one turn transfer matrix. For RHIC, β_1 and β_2 can be considerably larger than β_x, β_y by as much as 100% in the worse case found. However, the $x_{\max}$, $y_{\max}$ for a given initial x, x', y, y' are not simply related to β_1, β_2. To investigate $x_{\max}$, $y_{\max}$, the CDF, the coupling distortion function was introduced.

3. The Coupling Distortion Function

The coupling distortion function, CDF, describes $x_{\max}$, $y_{\max}$ for a given initial x, x', y, y'. The CDF at the point s is defined by

$$CDF = \frac{x_{\max}(s)}{x_{\max,\mathrm{nc}}(s)} \tag{3.1}$$

for a given initial x, x', y, y' at $s = s_o$. $x_{\max,\mathrm{nc}}$ is the $x_{\max}$ in the absence of coupling. For examining the loss in A_{SL}, $\epsilon_x = \epsilon_y$, $x' = y' = 0$ at the start is chosen. A corresponding CDF is defined for the y motion.

To compute CDF, one has to compute $x_{\max}(s)$ in the presence of coupling. An analytical result was found for $x_{\max}(s)$ in terms of β_1, β_2, ϵ_1, ϵ_2 and the R matrix. This result is given in Section 6.

Table 1 lists the coupling distortion function, CDF, and the β–functions of the normal modes, β_1 and β_2 for ten different distributions of the random field errors. The random quadrupole errors are described in section 7. The CDF is the largest CDF found at any of the high β quadrupoles in the insertions for either x or y motion for a particle starting at the focusing quadrupole in the middle of the first arc in RHIC. The β_1, β_2 are the largest β–functions of the normal modes found around the accelerator. For $a_1 = b_1 = 0$, the largest β functions are $\beta = 220$ m for $\beta^* = 6$ and $\beta^* = 630$ for $\beta^* = 2$. A CDF as large as CDF $= 2.1$ is found for one field error distribution. A simple picture of coupling would suggest CDF $\simeq 1.4$ resulting from a complete exchange of the emittance between the x and y motions. The betatron distortion is about 40% larger for the worst case than what one would expect from the simple picture of a complete exchange of the emittances.

Table 1. CDF at High β Quads

Field Error Number	$\beta^* = 6$			$\beta^* = 2$		
	CDF	β_1(m)	β_2(m)	CDF	β_1(m)	β_2(m)
1	1.47	246	236	1.32	695	684
2	1.38	266	264	1.46	650	644
3	1.29	237	244	1.30	682	744
4	1.52	254	249	1.55	723	797
5	1.48	255	260	1.10	766	752
6	1.43	230	223	1.38	625	654
7	1.67	250	224	2.10	956	970
8	1.71	305	284	1.63	816	764
9	1.33	237	243	1.30	687	655
10	1.33	255	248	1.35	797	670

There is some correlation between CDF and β_1 and β_2. However, the CDF depends not only on β_1, β_2 but also on the mismatch in the emittances. For the given initial ϵ_x, ϵ_y, the corresponding ϵ_1, ϵ_2 may be larger than ϵ_x, ϵ_y.

Table 2 shows the correlation between the CDF and the dynamic aperture which is measured by A_{SL}. A_{SL} is found from tracking studies with the random field errors, including higher multipoles, present. A_{SL} is the largest stable initial x with the starting conditions $\epsilon_x = \epsilon_y$, $x' = y' = 0$, and starting at the focusing quadrupole at the middle of the first arc in RHIC.

The correlation between the coupling distortion function, CDF, and the dynamic aperture A_{SL} is good. Note that the A_{SL} are computed after the coupling has been corrected[3] using the a_1 correctors at Q2 and Q5.

Table 2. Correlation of the CDF and A_{SL}

Field Error Number	$\beta^* = 6$		$\beta^* = 2$	
	CDF	A_{SL} (mm)	CDF	A_{SL} (mm)
1	1.47	14.5	1.32	8.5
2	1.38	14.5	1.46	6.5
3	1.29	15.5	1.30	8.5
4	1.52	15.5	1.55	7.5
5	1.48	14.5	1.10	8.5
6	1.43	16.5	1.38	8.5
7	1.67	12.5	2.10	4.5
8	1.71	12.5	1.63	6.5
9	1.33	16.5	1.30	8.5
10	1.33	14.5	1.35	7.5

[3] G. Parzen, AD/RHIC–AP–72 (1988).

In the absence of the random a_1, b_1, the stability limit has been found to be $A_{SL} = 15.5$ mm for $\beta^* = 6$ and $A_{SL} = 7.5$ mm for $\beta^* = 2$. The results in Table 2 indicate that for this particular starting place around the ring, A_{SL} has been reduced to $A_{SL} = 4.5$ mm for $\beta^* = 2$ m. The dependence of A_{SL} on the starting location around the ring is discussed in section 4.

The large CDF, CDF ~ 2 found above can be correlated with the nearby sum resonances $\nu_x + \nu_y = 58$ and $\nu_x + \nu_y = 57$. This is useful in finding a correction system to reduce the large CDF.

4. Azimuthal Dependence of CDF and A_{SL}

In the previous tables, CDF and A_{SL} were computed at the middle QF in the first inner arc in RHIC. If one computes CDF starting at different QF, CDF will change and thus A_{SL} will also change. β_1 and β_2 will also change.

If the particle is started at different QF, the value of CDF, A_{SL} and β_1, β_2 will change at each QF. Figure 1 shows this variation in CDF and β_1 at the 12 QF in the first arc. Roughly, CDF and β_1 oscillate around the ring. The CDF plotted is the largest CDF found at the high–β quadrupoles in the insertions, when the particle is started at different QF.

It is likely that A_{SL} will also oscillate around the ring, since A_{SL} and CDF are well correlated. In Fig. 2 A_{SL} is plotted versus CDF for a particle starting at 5 different QF in the ring. These 5 points include the largest and smallest CDF found in the ring. A_{SL} is computed at the QF at which the particle is started.

Since A_{SL} now depends on which QF the particle is started at, one has the problem of which value of A_{SL} is to be used for the dynamic aperture. The procedure used here is to find the average A_{SL} using the A_{SL} found at all the QF in the ring.

To compute $A_{SL,av}$ the average A_{SL}, one should in principle compute A_{SL} at all the QF in the ring and then compute the average A_{SL}. This would require a good deal of effort. Instead, the following procedure was used. The coupling distortion function at the high β quadrupole is computed starting at each QF in the ring. One then locates the QF that give the largest and smallest CDF, $\mathrm{CDF_{max}}$ and $\mathrm{CDF_{min}}$. The stability limit A_{SL} is computed starting at these two QF. It is assumed that this gives the largest and smallest A_{SL}, $A_{SL,max}$ and $A_{SL,min}$. The average A_{SL} is then computed as

$$A_{SL,av} = \frac{1}{2}(A_{SL,max} + A_{SL,min})$$

The computation of $A_{SL,av}$ for the two worst field errors, errors 7 and 8, are shown in Table 3.

Table 3. Computation of $A_{SL,av}$

β^*	Error No.	$A_{SL,max}$	$A_{SL,min}$	$A_{SL,av}$	CDF Max	CDF Min
6	7	14.5	11.5	13	1.67	1.29
6	8	16.5	10.5	13.5	2.0	1.24
2	7	8.5	4.5	6.5	2.1	1.10
2	8	8.5	6.5	7	1.8	1.21

The loss in A_{SL} is now 15%. A_{SL} has been decreased from 15.5 mm to 13 mm, for $\beta^* = 6$ from 7.5 mm to 6.5 mm for $\beta^* = 2$.

Figure 3 shows the maximum and minimum CDF found by starting at each QF in the ring for the ten different error distributions. The dashed line at CDF $= 1.414$ is the value of CDF expected using the simple picture of a complete exchange of ϵ_x and ϵ_y between the x and y motions. This plot shows that error distributions that do not show much loss in A_{SL} still may have a CDF appreciably larger than CDF $= 1.414$.

5. Loss in Linear Acceptance

The loss in linear acceptance due to the betatron distortion may be more serious than the loss in dynamic aperture. For injection the injected beam could be much larger because of the betatron distortion. For extraction, the extraction magnet could be off by quite a bit in its location in order to accept the required emittance of 6π. The correction of the betatron distortion (the CDF) appears important.

It may be possible to design an a_1 correction system that corrects the betatron distortion all around the ring. The system of separately excited a_1 near each Q2, previously proposed,[4] may correct this betatron distortion to a certain extent.

6. Analytical Results for $X_{\max}$ and $Y_{\max}$

In this section, analytical results are given for the maximum x and y, $x_{\max}$ and $y_{\max}$, that will be reached for a particle with a given initial x, x', y, y' in the presence of coupling. These results are needed in order to compute the coupling distortion function, CDF. Derivations of these results will be given in a future paper.

[4] G. Parzen, AD/RHIC/AP–89, 1990.

For a given set of initial x, x', y, y', x_{max} and y_{max} are given by

$$
\begin{aligned}
x_{\text{max}} &= (\beta_1 \epsilon_1)^{\frac{1}{2}} \cos\phi + (\beta_{x,2}\epsilon_2)^{\frac{1}{2}} \sin\phi , \\
\beta_{x,2} &= \bar{D}_{11}^2 \beta_2 + \bar{D}_{12}^2 \gamma_2 + 2\bar{D}_{11}\bar{D}_{12}\alpha_2 , \\
y_{\text{max}} &= (\beta_2 \epsilon_2)^{\frac{1}{2}} \cos\phi + (\beta_{y,1}\epsilon_1)^{\frac{1}{2}} \sin\phi , \\
\beta_{y,1} &= D_{11}^2 \beta_1 + D_{12}^2 \gamma_1 + 2D_{11}D_{12}\alpha_1 \ .
\end{aligned}
\tag{6.1}
$$

D and $\bar{D}$ are 2×2 matrices, which together with ϕ define the 4×4 R matrix, defined in section 2. R is given by

$$
R = \begin{pmatrix} I \ \cos\phi & D \ \sin\phi \\ -\bar{D} \ \sin\phi & I \ \cos\phi \end{pmatrix}
\tag{6.2}
$$

$\bar{D} = D^{-1}$, $|D| = 1$ and I is the 2×2 identity matrix.

β_1, α_1, γ_1 and β_2, α_2, γ_2 are the orbit parameters of the normal modes, ϵ_1 and ϵ_2 are the emittances of the normal odes that correspond to the initial x, x', y, y'.

One can also find expressions for x'_{max} and y'_{max}. These are given by

$$
\begin{aligned}
x'_{\text{max}} &= (\gamma_1 \epsilon_1)^{\frac{1}{2}} \cos\varphi + (\gamma_{x,2}\epsilon_2)^{\frac{1}{2}} \sin\phi , \\
\gamma_{x,2} &= \bar{D}_{21}^2 \beta_2 + \bar{D}_{22}^2 \gamma_2 + 2\bar{D}_{21}\bar{D}_{22}\alpha_2 , \\
y'_{\text{max}} &= (\gamma_2 \epsilon_2)^{\frac{1}{2}} \cos\varphi + (\gamma_{y,1}\epsilon_1)^{\frac{1}{2}} \sin\phi , \\
\gamma_{y,1} &= D_{21}^2 \beta_1 + D_{22}^2 \gamma_1 + 2D_{21}D_{11}\alpha_1 \ .
\end{aligned}
\tag{6.3}
$$

Edwards and Teng[2] describe how to compute the R matrix and β_1, α_1, γ_1 and β_2, α_2, γ_2 from the one turn transfer matrix. This then allows one to compute ϵ_1 and ϵ_2 from the initial x, x', y, y'. Equation 6.1 can then be used to compute x_{max} and y_{max} for the given initial x, x', y, y', which is needed to compute the coupling distortion function, CDF (see Eq. (3.1) for CDF).

7. Random a_1, b_1 Present in RHIC

The random quadrupole errors are due to a number of sources that include construction errors in the magnet coils, effective length errors in the quadrupoles, and rotational errors in the positioning of the quadrupoles.

a_1 and b_1 are defined so that the field due to a_1 and b_1 on the median plane is given by

$$
\begin{aligned}
B_y &= B_0 b_1 x \\
B_x &= B_0 a_1 x
\end{aligned}
$$

where B_0 is the main dipole field.

The rms random a_1, b_1 used in this study are given in the following table.

Source	$a_1/10^{-5}$ (cm^{-1})	$b_1/10^{-5}$ (cm^{-1})
Dipole coil error	16.8	8.4
Quadrupole coil error	15	15
Quadrupole effective length	—	40
Quadrupole rotation error	40	—

The assumed effective length error in the quadrupoles is $\Delta L/L = 2 \times 10^{-3}$ rms. The assumed rotational error in the quadrupoles is $\Delta\theta = 1 \times 10^{-3}$ rad rms.

Fig. 1. β_1 and CDF at different Q_F

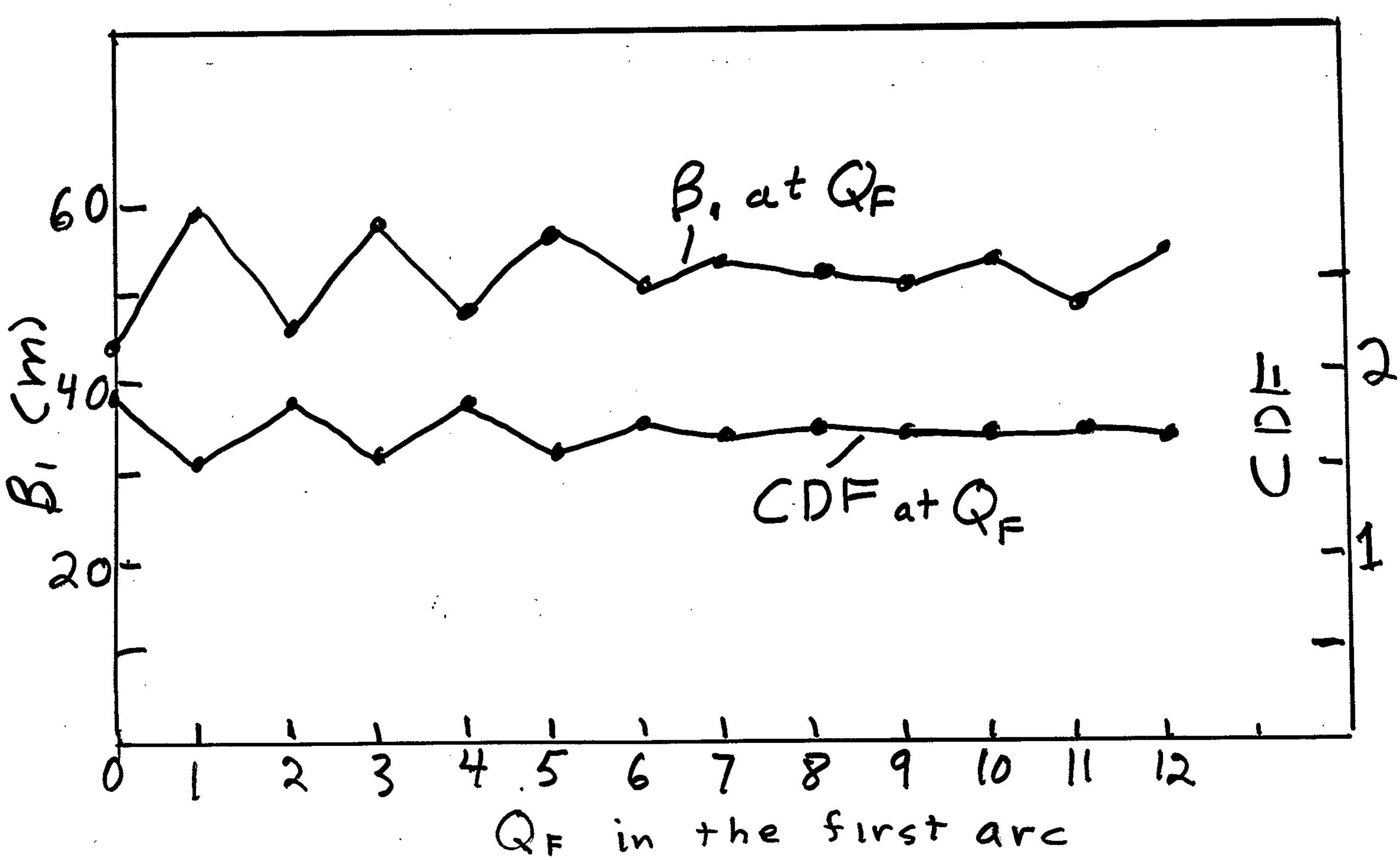

Fig. 2. Stability Limit, A_{SL}, versus CDF

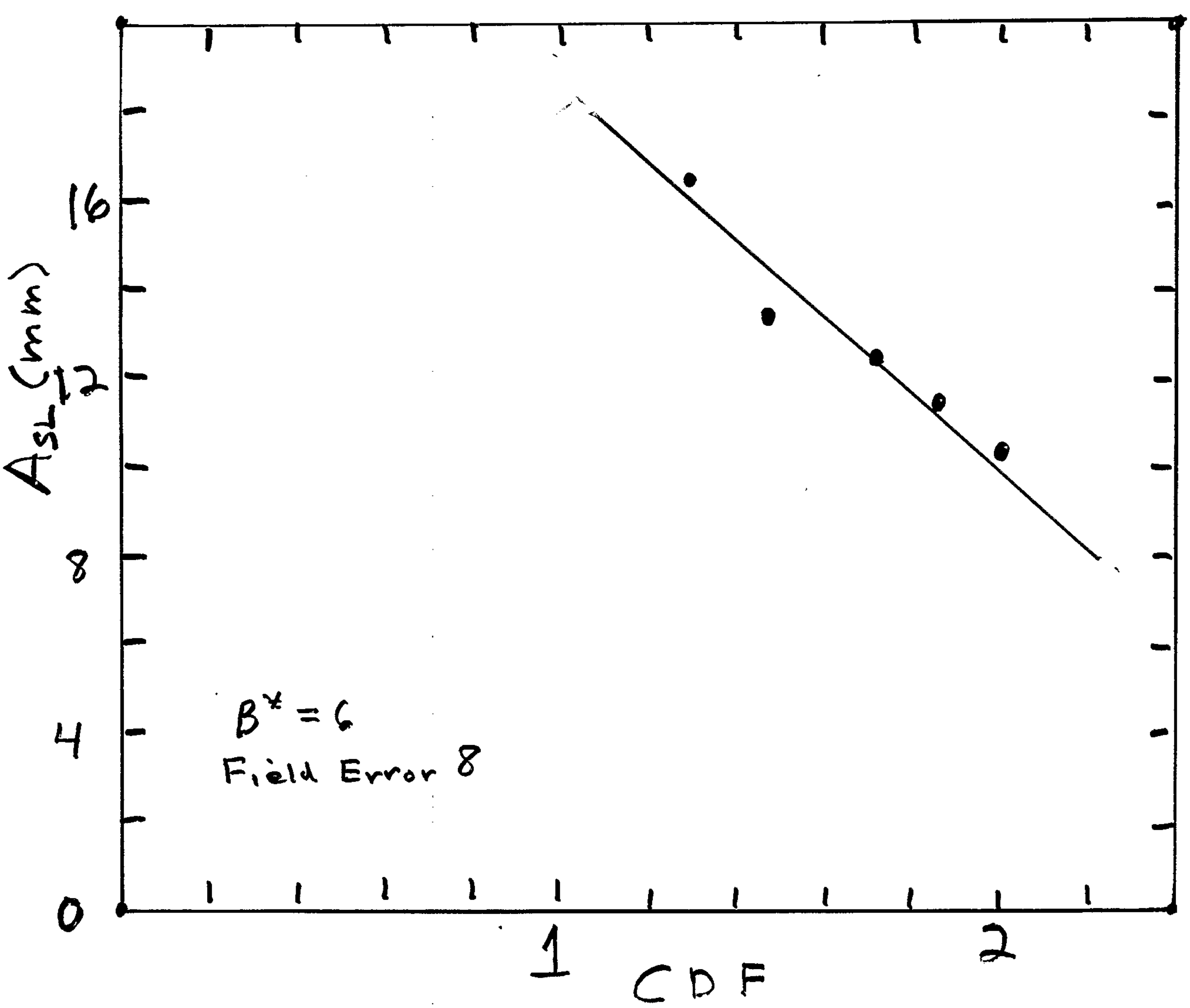

Fig 3. CDF for 10 Random Field Errors